PROCEEDINGS OF SCIENCE

Holistic study of space weather and space climate: 1700-2018

H.S. Ahluwalia [1]
University of New Mexico
Albuquerque, NM 87131, USA
E-mail: hsa@unm.edu

Abstract

We present an update of changes in space weather/space climate at Earth orbit using sunspot number (SSN) timeline (1700-2018), geomagnetic indices aa/Ap (1870–2018), solar polar magnetic field (1976-2017), interplanetary magnetic field (IMF) and galactic cosmic ray (GCR) flux (1963-2018) in the stratosphere at high latitudes. The Cycle 24 is close to minimum, expected in 2020. The baseline of aa index increases monotonically from 1900 to 1986 declining steeply afterwards, solar polar magnetic field decreases systematically for last three cycles (22–24) as do SSNs at cycle peaks. Livingston and Penn (2009) note a long term weakening of maximum magnetic field in sunspots since 1992. They expect SSNs for the Cycle 25 to peak at 7 (a steep decline in solar activity) leading to Maunder-like minimum, in contrast to prediction of a Dalton minimum by several colleagues. The North-South asymmetry in the solar polar field is pronounced for the decay phase of cycles 23, 24, it seems to change sign after the Cycle 21. GCR flux in the stratosphere is higher than in 1965 and increasing, pointing to an enhanced radiation exposure in future for passengers on transpolar flights, the astronauts on the space station as well as those travelling to and staying on the Moon and the Mars on prolonged missions; the assets in space would have to be hardened for safety from enhanced radiation.

36th International Cosmic Ray Conference -ICRC2019-
July 24th - August 1st, 2019
Madison, WI, U.S.A.

[1] Speaker

PoS(ICRC2019)1048

1. Introduction

The Sun controls space weather with geo-effective fast coronal mass ejections (fCMEs) increasing radiation in space (Ahluwalia, 2015a); CME frequency corresponds with sunspot number (SSN) cycles (Gosling et al., 1991; Webb and Howard, 1994; Gopalswamy et al., 2003). Wang and Colaninno (2014) report that high speed (> 350 km/s) CME rate observed with Large Angle Spectrometric Coronagraph for 1996-2013 follows SSN timeline (cc = 0.90) implying that weaker cycles will produce fewer fCMEs. The average period of SSN cycle is 11.2y, actual periods have ranged from 7 to 14y (Kane, 2008). Balasubramanium and Henry (2016) describe a procedure for converting locally observed sunspot drawings obtained with the U.S. Air Force Improved Solar Optical Observing network (ISOON) to international SSNs. Clette et al. (2014) revised the international SSN timeline since its creation by Wolf in 1849 starting in 1700 and ending in May 2015; the data are available at WDC-SILSO, Royal Observatory of Belgium at Brussels (silso.obs@oma.be). Ahluwalia and Ygbuhay (2016) discuss the salient features of new SSN series SSN(V2). In this paper we update the evolution of SSN(V2) timeline and space weather /space climate for several cycles using geomagnetic indices aa/Ap, solar polar field, IMF and GCR flux in the stratosphere, inferring that we do not yet fully understand how the solar dynamo operates; a study of the next two cycles (25, 26) may help enhance our understanding.

2. SSN(V2)

Fig. 1 depicts SSN(V2) timeline. The updated annual mean SSNs are plotted in black for 1700-2018; every fourth cycle is labeled bold, showing that the Sun is a variable magnetic star with phases of enhanced activity followed by those of low activity (Eddy, 1976, 1981). The grand minima are indicated, namely the 70y Maunder minimum (1645–1715, MM) named after the astronomer Edward Maunder, the 40y Dalton minimum (1790–1830, DM) named after the meteorologist John Dalton, the shallow 13y Gleissberg minimum (1889–1902, GM). One notes:

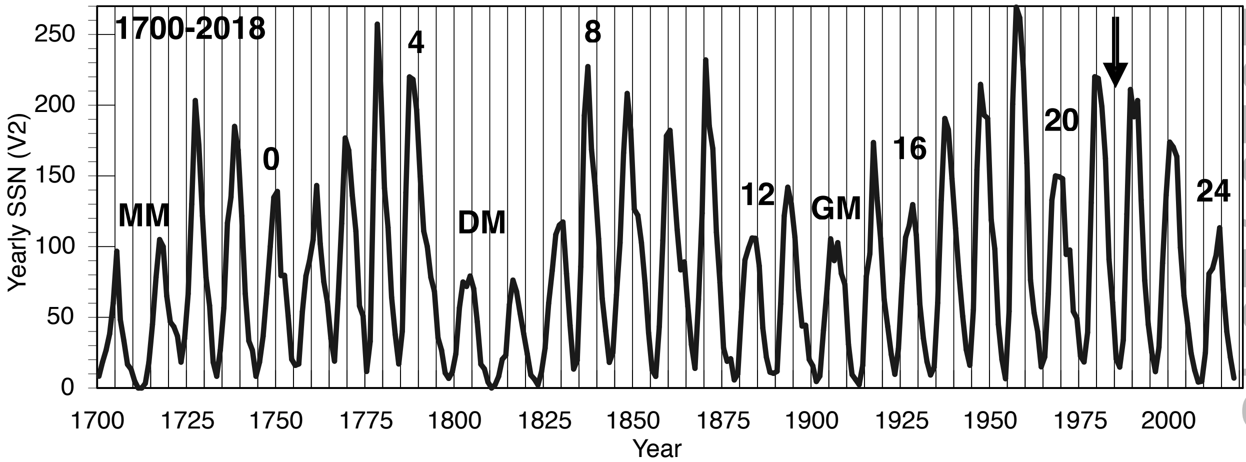

Fig. 1 depicts updated SSN(V2) timeline for 1700-2018; see text for details.

1. The Cycle 3 is about as active as the Cycle 19 (the most active cycle ever recorded); two cycles are 175y (~2 x Gleissberg period) apart. Mean SSN for the covered period is 79.5.
2. Beginning with the well observed Cycle 10 (McKinnon, 1987; Wilson, 1987), there is a pattern where even cycle of the even–odd pairing is less active (Gnevyshev and Ohl,1948), it disappears after cycle 21; the physical process(es) leading to these solar features are not understood.
3. The Sun entered a period of low solar activity at the minimum of the Cycle 21, shown by the downward pointing arrow. Until the Cycle 23 SSN was above average but for the Cycle 24 it is below average, reaching activity level closer to that in early 1900s but it has not reached minimum yet. Ahluwalia and Ygbuhay (2012) suggest that we may be at the advent of a Dalton-like minimum which lasted 40y, in agreement with some colleagues (Stozhkov et al., 2013; Steinhilber and Beer, 2013; Gkana and Zachilas, 2016; Kirov et al., 2018) but De Jager and Duhau (2012) state that no grand minimum is expected to occur in the 21st century, Lockwood (2010) opines there is only 8% chance of the Sun falling into a grand minimum in the next 40 years but Lockwood et al. (2018) expect Dalton minimum to occur in 2050. Penn and Livingston (2010) suggest that SSNs for the Cycle 25 will peak at 7 (a steep decline in solar activity) leading to a Maunder-like minimum, compared to our prediction of a Dalton minimum. In contrast, Pesnell and Schatten (2018) infer that the Cycle 25 will be comparable to the Cycle 24; the peak

may occur near 2025.2 ± 1.5 year.

4. The timeline for the Cycle 24 has an unusual structure. Its amplitude is quite small, and it is moving slowly towards minimum expected circa 2020. Also, it has two peaks, the first in 2012 due to activity in the north hemisphere (NH) and a second higher peak in 2014 due to an excess activity in SH (Ahluwalia, 2016). There are more sunspots in NH for 1950-1970 and excess sunspots in SH for descent of cycles 21-23 (1980-2010) more so for the Cycle 24 decay phase (Svalgaard and Kamide, 2013; Ahluwalia, 2015b, 2016). Murakozy and Ludm´any (2012) analyzed hemispheric SSN data from the Greenwich Royal Observatory for 12 cycles (12-23), finding phase of hemispheric cycles shows an alternating variation; NH leads in 4 and follows in 4 cycles, 4+4 cycle period is close to Gleissberg (1939) cycle; Zolotova et al. (2009) reached a similar conclusion. Vernova et al. (2014) find that the Cycle 24 may be violating this rule.

3. Solar polar magnetic field

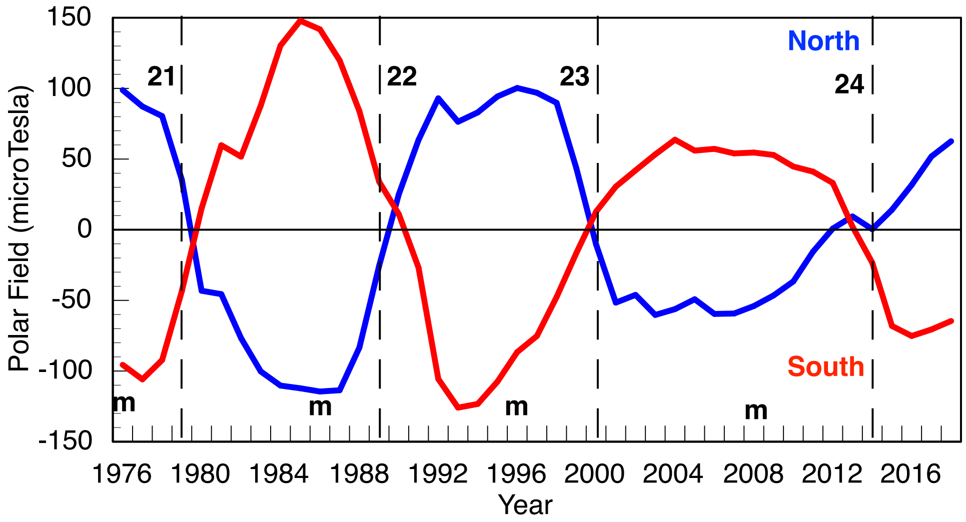

Fig. 2 depicts updated solar polar field data for 1976-2018; see text for details.

Yearly updated solar polar magnetic field for 1976-2018 is plotted in Figure 2. The data are available at the Wilcox Solar Observatory (WSO) website: http://quake.stanford.edu. They cover three cycles (21-23) and parts of the other two (20, 24). The vertical dashed lines indicate SSN maximum, m indicates minimum. One notes the following:

1. Polar field (PF) reaches maximum near the SSN minimum in both hemispheres. For a spotless Sun, IMF (**B**) is sustained by contributions from PF. In SH it reached a maximum value for the Cycle 24 in 2016 and is beginning to level-off in NH in 2018, indicating that we may be near the Cycle 24 minimum.
2. PF reversals occur after SSN maximum for cycles 21, 22 and before SSN maximum for the Cycle 24. It is not clear why.
3. N-S asymmetry in PF is most pronounced for the decay phase of cycles 23, 24; it seems to change sign after the Cycle 21.
4. PF change in NH for the ascent of even cycle 22 (1984-1992) is larger but decreases systematically for the last three cycles (22-24), a trend seen in SSNs (see Fig. 1) also. It is likely to continue into the future. Livingston and Penn (2009) noted a long term weakening of the maximum sunspot field since 1992. They expect SSNs for the Cycle 25 to peak at 7 (a steep decline in solar activity) leading to a Maunder-like minimum.

4. B and GCR ions

In situ measurements of B and V at 1AU started in October 1963 [Snyder et al., 1963] at the dawn of the space age. SSNs bear a positive correlation with B (Ahluwalia, 2013) and a negative correlation with GCRs (Forbush, 1966). GCR ions observed with balloons at high latitudes (Bazilevskaya et al., 2012) for 1963-2018 are plotted in Fig. 3a, data are normalized to 100% in 1965; median rigidity of response (Rm) to GCR rigidity spectrum for ion detector on balloons ~ 4 GV, positive (p) and negative (n) polarity intervals are covered when **B** is outward/ inward from the Sun; solar magnetic polarity changes sign near

SSN maximum. The data span four complete sunspot cycles (20-23) and part of the Cycle 24. A negative correlation is clearly seen between GCR ions and B. In particular, note the upward GCR trend (shown by dashes) after the Cycle 22, they recovered to the highest level at the Cycle 23 minimum in 2009 and exceed the 1965 level in 2018 but the Cycle 24 has not reached minimum yet. Note the following

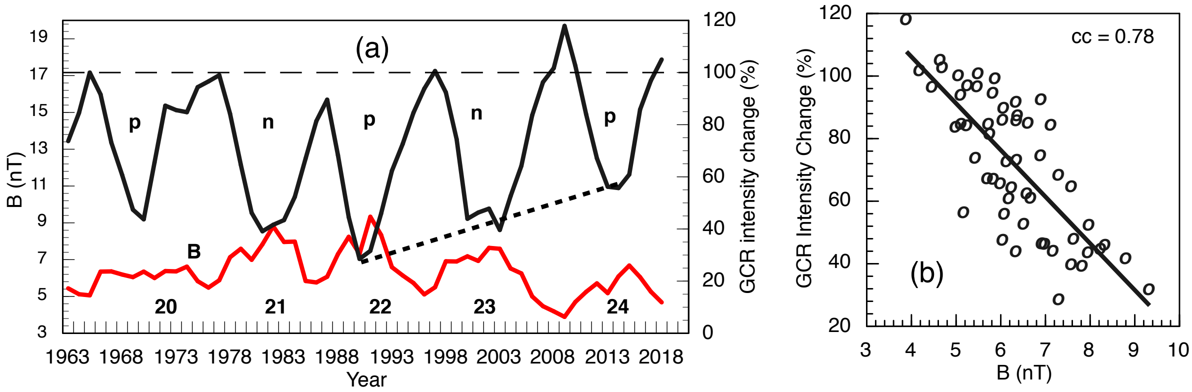

Fig. 3a depicts a plot of B and GCR ions for 1963-2018, and 3b depicts linear correlation between GCRs (%) and B (nT), p/n intervals are indicated.

features:

- B is flat at ~ 6.5 nT for the Cycle 20 but exhibits 11y cycle later. It has two peaks, one near SSN max due to ICMEs and a post-max higher peak due to coronal high-speed streams (HSS).
- After cycle 20, min B has smaller values for each cycle, reaching the smallest value ever measured in the space age in 2009 at the Cycle 23 min (of long duration), corresponding to a similar trend in SSN minima. One may ask how low B would be circa 2020 and how long it would stay at the low level.
- The correlation between GCRs (%) and B (nT) depicted in Fig. 3a is displayed in Fig. 3b. The linear fit has a correlation coefficient (cc) = 0.78. The regression relation is:

$$\text{GCR ions (\%)} = -15^*\text{B (nT)} + 166 \qquad (1)$$

McCracken (2007) estimates IMF ~ 1nT in 1900 (see his Fig. 4), implying that GCR flux in the stratosphere may reach higher values circa 2020 compared to that in 2009 (if B drops to 1 nT) resulting in an enhanced radiation exposure for the passengers on transpolar flights, the astronauts on the space station and those travelling to the Moon and the Mars on long duration missions; the assets in space may also have to be hardened for safety. Schwadron et al. (2014) reached similar conclusions using data from the Cosmic Ray Telescope for the Effects of Radiation (CRaTER). They compute radiation dose based on estimated values of the solar modulation potential (Φ) derived by Gleeson and Axford (1968) invoking a spherical symmetry of the Parker equation (1965). Ahluwalia et al. (2015) show that use of Φ does not explain empirical results of their analyses of neutron monitor data from global network (Rm ~ 20 GV); so their estimates of the radiation dose increase should be treated with caution.

5. Planetary indices Ap, aa and SSN(V2)

Updated planetary index Ap data are plotted in Fig. 4; Ap was designed by Bartels (1962) to measure the geo-effectiveness of HSS. The index has a linear scale and is derived from data at mid-latitude geomagnetic observatories (Mayaud, 1980); Ap ∝ VB, solar wind velocity (V) fluctuates about 450 km/s so Ap is affected by a long-term trend in B; data are available at: http://www.ngdc.noaa.gov. Ahluwalia (2000, 2003, 2011, and references therein) discovered a three-cycle quasi-periodicity (TCQP) in Ap and B. He devised an empirical method to predict smooth SSNs at peak (Rmax) and rise time (Tr) of a cycle, leading to a successful prediction for the Cycle 23 (Kane, 2008; Petrovay, 2010). TCQP is depicted in Fig. 4 by dashes for an extended period (1932-2018); its slope turns sharply negative after 1988.

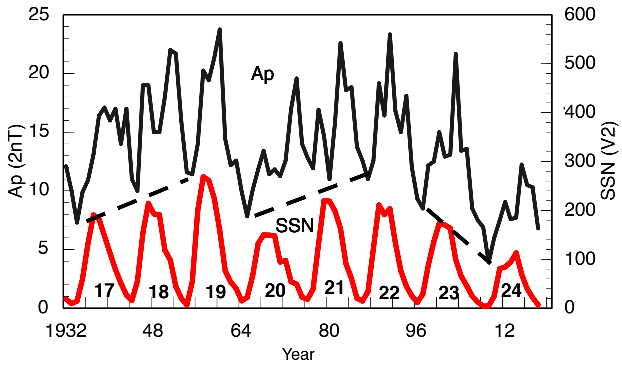

Fig. 4 depicts updated yearly Ap, SSN(V2) for 1932-2018; TCQP is highlighted by dashes.

Ahluwalia and Jackiewicz (2011, 2012) used the same method to predict the peak for the Cycle 24 to be about half of the Cycle 23 Rmax with Tr = May 2013 ± 6 months; excess activity in SH was not anticipated by them (Ahluwalia, 2016). We cannot forecast Rmax and Tr for the Cycle 25 until about 2021. Yearly SSN(V2) are also plotted in Fig. 4; maxima occur in 1937, 1947, 1957, 1968,1980, 1989, 2000, 2014 and minima in 1933, 1944, 1955, 1965, 1976, 1986, 1996, 2008. A descending trend in SSN peaks is noted beginning with the Cycle 22; it is likely to continue into the future. Livingston and Penn noted a long term weakening of max sunspot field since 1992. They predict the Cycle 25 will peak with 7 sunspots, implying that we may be on the verge of a Maunder-like minimum in contrast to our prediction of a Dalton minimum.

Fig. 5 shows yearly plot of aa index and SSN(V2) for 1870–2018, for twelve cycles (12-23) and parts of other two (11, 24); data are an updated version of a compilation by Mayaud (1972, 1973) from data obtained at two old magnetic observatories, Greenwich and Melbourne; Ap, aa bear a linear correlation (Mayaud, 1980). The following features are noted:

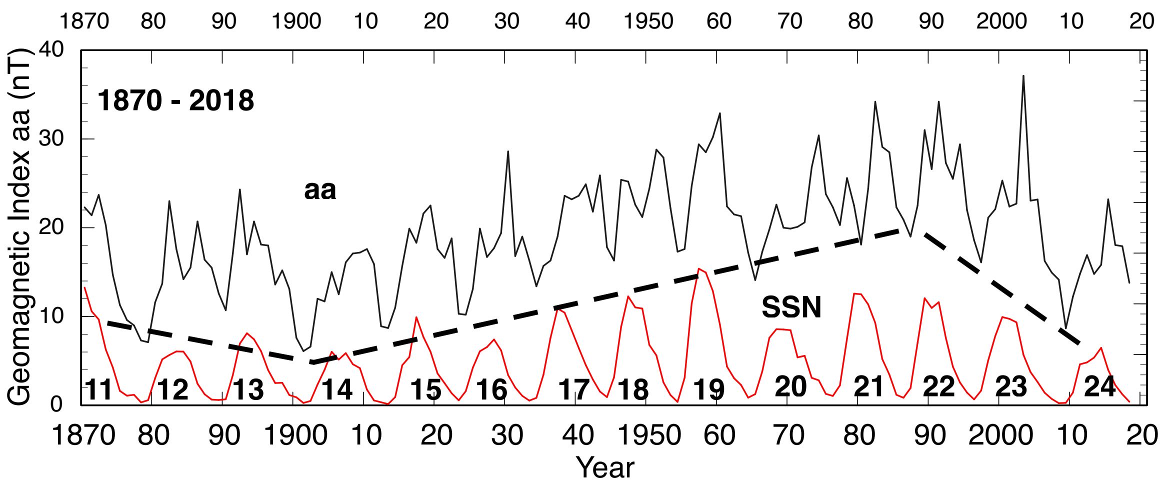

Fig. 5 depicts updated yearly values of the aa index and SSN(V2) for 1870–2018.

1. Beginning in 1900 an upward trend exists in aa for the 20th century, undergoing TCQP for cycles 14-21. Silverman (1992) used 45, 000 observations of monthly auroral occurrence to obtain a power spectrum showing significant power at periods 83, 55, 33.3, 11.1 years. Alicia et al. (1993) did a power spectrum analysis of monthly Ap data for 1932-1982 showing significant power at 10.2, 32.1 years, noting that TCQP is very unstable it also occurs in other data (Ahluwalia, 2012).
2. The slope of aa timeline changes from negative to positive near the Cycle 13 minimum in 1900 and from positive to negative near the Cycle 21 minimum (1986) as is the case for Ap in Fig. 4; the interval of 86 years corresponds to the Gleissberg cycle. The steeper slope during the last few solar cycles compared to that of the period before 1900 indicates that aa/Ap timeline may reach a level closer to DM

level in the 21st century (Ahluwalia 2016), undergoing TCQP until an uptick occurs in the seventies; the reader is alerted to the fact that no understanding exists of a relation between TCQP and solar dynamo mechanism. If TCQP does not continue beyond 2020, our predictions for future SSNs will come under scrutiny, with implications for future space weather / space climate. We are unable to forecast the degree and the change of sign of N-S asymmetry in PF because the physics of the origin of N-S asymmetry in the dynamo operation is not understood. In light of these issues it would instructive to see how the Cycles 25, 26 develop.

6. Conclusions

Evolution of space weather / space climate is explored heuristically for 1870-2018. We still do not fully understand the solar dynamo mechanism (Parker, 2009). For example, we do not understand how TCQP is related to the dynamo operation nor do we understand how N-S asymmetry arises and evolves. We do have an opportunity to learn a great deal more about the dynamo operation with the study of the next two cycles (25, 26). Our investigation leads to the following conclusions:

1. PF is decreasing in NH for the last three cycles (22-24), the decline is likely to continue into future. Livingston and Penn (2009) noted a long term weakening of maximum sunspot field since 1992. They predict that SSNs for the Cycle 25 will peak at 7, indicating the advent of a Maunder-like minimum, in contrast to our prediction of a Dalton minimum.
2. PF in SH seems to have reached its maximum value for the Cycle 24 in 2016 and it seems to be flattening in NH in 2018, indicating that we may be near the cycle minimum. We are unable to forecast the degree and future change of sign of N-S asymmetry in PF since no understanding exists how it comes about and evolves.
3. The good news is that we are sailing into a fair space weather/space climate when the frequency of fCMEs and storm sudden commencements (SSCs) will be sharply reduced decreasing the risk to electrical installations at high latitude locations on the Earth. Even so, an occurrence of the magnetic storm of 1859 (Tsurutani et al., 2003) cannot be ruled out.
4. The bad news is that radiation exposure due to an increase in GCRs (rather than solar activity) may be enhanced for passengers on transpolar flights, astronauts on the space station and those travelling to the Moon and the Mars on long duration missions. The assets in space will have to be hardened for safety from increased radiation. Schwadron et al. (2014) reached similar conclusions using data of the Cosmic Ray Telescope for the Effects of Radiation (CRaTER).

Acknowledgements

I thank Frederic Clette for revised international sunspot number data, Galina Bazilevskaya for the high latitude balloon record of GCR ions, the providers of the solar and interplanetary data and Roger Ygbuhay for technical assistance. I am grateful to U.S. Air Force Office of Scientific Research for the award of the Summer Faculty Research Fellowship at the Space Vehicles Directorate, Kirtland Air Force Base, NM, for 2018 and 2019.

Data sources: WDC-SILSO, Royal Observatory of Belgium at Brussels (silso.obs@oma.be); Wilcox Solar Observatory (WSO) website: http://quake.stanford.edu; Ap, B data are available at: http://www.ngdc.noaa.gov.

References

Ahluwalia, H.S. Ap time variations and IMF. J. Geophys. Res., 105, 27481–27487, 2000.

Ahluwalia, H.S. Meandering path to solar activity forecast for cycle 23. Velli, M., Bruno, R., and Malra, F. (Eds.), Solar wind Ten: Proc.10th Int. Solar Wind Conf., AIP: CP679, pp. 176–179, 2003.

Ahluwalia, H.S., and J. Jackiewicz. Sunspot cycle 24 ascent to peak activity: a progress report. Proc. 32nd Int. Cosmic Ray Conf., 11, 232–234, 2011.

Ahluwalia, H.S. Timelines of cosmic ray intensity, Ap, IMF, and sunspot numbers since 1937. J. Geophys. Res., 116, A12106, 6 pp., 2011.

Ahluwalia, H.S. Three-cycle quasi-periodicity in solar, geophysical, cosmic ray data and global climate change. Indian J. Radio & Space Phys., 41, 509-519, 2012.

Ahluwalia, H.S., and J. Jackiewicz. Sunspot Cycle 23 descent to an unusual minimum and forecasts for cycle 24 activity. Adv. Space Res. 50, 662–668, 2012.

Ahluwalia, H.S., and R.C. Ygbuhay. Sunspot cycle 24 and the advent of Dalton-Like minimum. Advances in Astronomy, http://dx.doi.org/10.1155/2012/126516, paper ID126516, 2012.

Ahluwalia, H.S. Sunspot numbers, interplanetary magnetic field, and cosmic ray intensity at earth: Nexas for the twentieth century. Adv. Space Res. 52, 2112–2118, 2013.
Ahluwalia, H.S. Unusual structure of sunspot cycle 24. 34th Int. Cosmic Ray Conf., The Hague, The Netherlands, 2015a.
Ahluwalia, H.S. North–south excess of hemispheric sunspot numbers and cosmic ray asymmetric solar modulation. Adv. Space Res., 56, 2645-2648, 2015b.
Ahluwalia, H. S., R. C. Ygbuhay, R. Modzelewska, L. I. Dorman, and M. V. Alania. Cosmic ray heliospheric transport study with neutron monitor data. J. Geophys. Res., Space Phys., 120, 8229– 8246, 2015.
Ahluwalia, H.S. and R. C. Ygbuhay. Salient features of the new sunspot number time series. Solar Phys., 291, 3807-3815, 2016.
Ahluwalia, H.S. The descent of the solar cycle 24 and future space weather. Adv. Space Res., 57, 710-714, 2016.
Alicia, L. C. G., W.D., Gonzales, S.L.G., Dutra, and B.T. Tsurutani. Periodic variation in the geomagnetic activity: A study based on the Ap index. J. Geophys. Res., Space Phys., 98, 9215– 9231, 1993.
Balasubramanium, K.S., and T.W. Henry. Sunspot numbers from ISOON: A ten-year data analysis. Solar Phys., 16 pp., Sunspot number calibration, DOI 10.1007/s11207-016-0874-5, 1993.
Bartels, J. Collection of Geomagnetic Planetary Index Kp and Derived Daily Indices Ap and Cp for the Years 1932–1961, 1962. North-Holland, New York.
Bazilevskaya, G.A., et al. Change in the rigidity dependence of the galactic cosmic ray modulation in 2008-2009. Adv. Space Res. 49, 784-790, 2012.
Clette, F., L., Svalgaard, J.M.,Vaquero, and E.W. Cliver, Revisiting the sunspot number: a 400-year perspective on the solar cycle. Space Sci. Rev., 186, 35-103, 2014.
De Jager, C., and S. Duhau. Sudden transitions and grand variations in the solar dynamo, past and future. J. Space Weather & Space Clim. 2, A07, 8pp, 2012. http://dx.doi.org/10.1051/swsc/2012008.
Eddy, J.A. The Maunder minimum. Science 192, 1189–1202, 1976.
Eddy, J.A. Climate and the role of the sun, Climate and History: Studies in interdisciplinary history in Rotberg R.I., and Rabb T.K. (Eds.), Princeton University Press, Princeton, New Jersey, p. 145, 1981.
Forbush, S.E. Time variations of cosmic rays. Handbuch der Physik, XLIX/1, Geophysics III, Part 1. Ed. S. Flugge, Springer-Verlag, Berlin-Heidelberg-New York, pp. 159-247, 1966.
Gkana, A., and L. Zachilas. Re-evaluation of predictive models in light of new data: Sunspot number version 2.0. Solar Phys, 291, 2457–2472, 2016. DOI 10.1007/s11207-016-0965-3.
Gleeson, L. J., and W. I. Axford. Solar modulation of galactic cosmic rays, Astrophys. J., 154, 1011-1026, 1968, doi:10.1086/149822.
Gliessberg, W. A long periodic fluctuation of the sunspot numbers. Observatory, 62, 158-159, 1939.
Gnevyshev, M.N., and A.I. Ohl. On the 22-year solar activity cycle. Astron, Z., 25, 18-20, 1948.
Gopalswamy, N., A. Lara, Y. Yashiro, and R.A. Howard. Coronal mass ejections and solar polarity reversal. Astrophys. J., 598, L63–L66, 2003.
Gosling, J.T., D.J. McComas, J.L. Phillips, and S.J. Bame. Counterstreaming solar wind halo electron events: solar cycle variations. J. Geophys. Res., 97, 6531-6535, 1991.
Kane, R.P. Prediction of solar cycle 24 based on the Gnevyshev-Ohl-Kopecky rule and the three-cycle periodicity scheme. Ann. Geophys., 26, 3329–3339, 2008.
Kirov, B., S. Asenovski, K. Georgieva, V.N. Obridko, and G. Maris-Muntean. Forecasting the sunspot maximum through an analysis of geomagnetic activity. J. Atmos. Solar-Terr. Phys., 176, 42-50, 2018.
Livingston, W. and M. Penn. Are sunspots different during this solar minimum? EOS, 90, 30, 2009.
Lockwood, M. Solar change and climate: an update in the light of the current exceptional solar minimum. Proc. R. Soc. A 466, 303–329, 2010. http://dx.doi.org/10.1098/rspa.2009.0519.
Lockwood, M., M. J. Owens, L. A. Barnard, C. J. Scott, C. E. Watt and S. Bentley. Space climate and space weather over the past 400 years: 2. Proxy indicators of geomagnetic storm and substorm occurrence. J. Space Weather & Space Clim., 8 (A12), 1-19, 2018.
Mayaud, P.N. The aa indices: A 100-year series characterizing the magnetic activity. J. Geophys.

Res. 77, 6870–6874, 1972.
Mayaud, P.N. A hundred-year series of geomagnetic data, 1868-1967, *IAGA Bull. 33*, Int. Union of Geod. and Geophys. Paris, 1973.
Mayaud, P.N. Derivation, meaning, and use of geomagnetic indices, Geophysical Monograph 22, American Geophysical Union, Washington, 1980.
McCracken, K.G. Heliomagnetic field near Earth:1428-2005. J. Geophys. Res., 112, A09106, 9pp, doi:10.1029/2006JA012119, 2007.
McKinnon, J.A. Sunspot numbers 1610-1985, World Data Center A for Solar-Terrestrial Physics, Boulder, CO. Report UAG-95, pp.1-105, 1987.
Murakozy, J., and A. Ludm´any. Phase lags of solar hemispheric cycles. Mon. Not. R. Astron. Soc., 419, 3624–3630, 2012.
Parker, E. N. Passage of energetic particles through interplanetary space, Planet. Space Sci., 13, 9–49, 1965.
Parker, E.N. Solar Magnetism: The state of our knowledge and ignorance. Space Sci. Rev., 144, 15-24, 2009.
Penn, M., and W. Livingston. Long-term evolution of sunspot magnetic fields. **arXiv:1009.0784**v1 [astro-ph.SR] 3 Sep 2010.
Pesnell, W.D., and K. H. Schatten. An early prediction of the amplitude of solar cycle 25. Solar Phys., 293: 112 (10 pp), 2018.
Petrovay, K. Solar cycle prediction. Living Rev. Solar Phys., 7, 5–59, 2010.
Schwadron, N. A., et al. Does the worsening galactic cosmic radiation environment observed by CRaTER preclude future manned deep space exploration? Space Weather, 12, 622-632, 2014.
Silverman, S.M. Secular variations of the aurora for the past 500years. Rev. Geophys., 30, 333-351, 1992.
Snyder, C. W., M. Neugebauer, and U. R. Rao (1963), The solar wind velocity and its correlation with cosmic ray variations and with solar and geomagnetic activity, J. Geophys. Res., 68, 6361–6370, doi:10.1029/JZ068i024p06361.
Steinhilber, F., and J. Beer. Prediction of solar activity for the next 500 years. J. Geophys. Res., 118, 1861–1867, 2013.
Stozhkov, Y., V. Okhlopkov, V. Makhmutov, and V. Logachev. Solar activity, cosmic rays, and global climate change. 33rd Int. Cosmic Ray Conf., Rio de Janeiro, Brazil, 2013.
Svalgaard, L., and Y. Kamide. Asymmetric solar polar field reversals. Astrophys J., 763 (issue 1), article id. 23 (6 pp), 2013.
Tsurutani, B.T., W.D. Gonzalez, G.S. Lakhina, and S. Alex. The extreme magnetic storm of 1-2 September 1859. J. Geophys. Res., 108, A7 (8 pp.), 2003.
Vernova, E.S., M.I. Tyasto, and D.G. Baranov. Photospheric magnetic field: Relationship between north-south asymmetry and flux imbalance. Solar Phys., 289, 2845-2865, 2014.
Wang, Y.M., and R. Colaninno. Is solar cycle 24 producing more coronal mass ejections than cycle 23? Astrophys. J., 784: L27 (7 pp), 2014.
Webb, D.F. and R.A. Howard. The solar cycle variation of coronal mass ejections and the solar wind mass flux. J. Geophys. Res., 99, 4201– 4220, 1994.
Wilson, R.M. On 'bimodality of the solar cycle' and the duration of cycle 21. Solar Phys., 108, 195–200, 1987.
Zolotova, N. V., D. I. Ponyavin, N. Marwan, and J. Kurths. Long-term asymmetry in the wings of the butterfly diagram. Astron. & Astrophys, 503, 197-201, 2009. DOI:10.1051/0004-6361/200811430.

PoS(ICRC2019)1048